Surface Active and Association Behavior of Oxybutylene–Oxyethylene and Oxyethylene–Oxybutylene–Oxyethylene Copolymers in Aqueous Solutions

ARTICLE *in* LANGMUIR · MAY 2003

Impact Factor: 4.46 · DOI: 10.1021/la027072j

3 AUTHORS, INCLUDING:

Saurabh Sureshchandra Soni
Sardar Patel University
37 PUBLICATIONS **547** CITATIONS
SEE PROFILE

Nandhibatla V Sastry
Sardar Patel University
72 PUBLICATIONS **1,459** CITATIONS
SEE PROFILE

Research Article

Surface Active and Association Behavior of Oxybutylene–Oxyethylene and Oxyethylene–Oxybutylene–Oxyethylene Copolymers in Aqueous Solutions

S. S. Soni, N. V. Sastry, John George, and H. B. Bohidar

Langmuir, **2003**, 19 (11), 4597-4603• DOI: 10.1021/la027072j • Publication Date (Web): 02 May 2003

Surface Active and Association Behavior of Oxybutylene−Oxyethylene and Oxyethylene−Oxybutylene−Oxyethylene Copolymers in Aqueous Solutions

S. S. Soni, N. V. Sastry,* and John George

Department of Chemistry, Sardar Patel University, Vallabh Vidyanagar 388 120, Gujarat, India

H. B. Bohidar

School of Physical Sciences, Jawaharlal Nehru University, New Delhi 110 067, India

Received December 26, 2002. In Final Form: February 26, 2003

The surface active and association properties of commercial diblock B_9E_{16} and triblock $E_{43}B_{14}E_{43}$ copolymers from Dow Chemical Company were measured from surface tension, dynamic light scattering, and viscosity data. The values of critical micelle concentrations, surface active properties, and the micellar size and its temperature dependence have been found to be distinct in both the copolymers which differ in the ratio of hydrophobic to hydrophilic block lengths. The noted increase in the micellar size and distortion in the shape of the micelles of diblock copolymer with temperature rise have been explained considering the dehydration of micelles at elevated temperatures. An attempt has also been made to relate the distinct differences in the dilute solution phase diagrams to the changes in micellar dimensions.

1. Introduction

Water soluble amphiphilic polymeric surfactants have received enormous attention and popularity because of their unique solution behavior and wide usage in a variety of applications. The hydrophilic part in these substances invariably has been poly(oxyethylene), PEO (E).[1] The hydrophobic part of the molecules offers a wider choice because it can be chosen from water insoluble long alkyl chains, poly(oxypropylene), PPO (P), poly(oxybutylene), PBO (B), poly(dimethylsiloxane), PDMS, polystyrene, PS, etc. Well-defined hydrophobic−hydrophilic copolymers based on EP, EB diblock and EPE, EBE, PEP, and BEB triblocks have been synthesized, and some of them are now commercially available. The architectural variation for a given composition or variable compositions within a given architecture enables these polymeric surfactants to possess unique phase, surface active, association, and gelation behaviors. These special features have been the subject of extensive academic investigations especially in dilute as well as concentrated solutions of EPE, EP, and PEP copolymers, and the published work has been reviewed by Chu and Zhou,[2] Alexandridis,[3] and Booth and Attwood.[4] Because of an inherent transfer reaction (hydrogen abstraction) involving propylene oxide monomer, the synthesized EPE triblock copolymers have been found to be compositionally heterogeneous and contain a significant proportion of diblock PE copolymers and also homopoly(oxypropylene). To over come this problem Heatley et al.[5,6] and Mai et al.[7] have selected 1,2-butylene oxide and styrene oxide as precursor monomers for the hydrophobe and found that the transfer reaction is absent when these monomers are copolymerized together with oxyethylene chains. Dow Chemical Company has made available a series of EB and EBE copolymers commercially.[8]

EB diblock copolymers are less hydrophobic than nonyl phenol and fatty alcohol ethoxylates but more hydrophobic than EP copolymers. Nace et al.[9] have reported that EB diblock copolymers have improved surfactant performance over their EP analogues. Distinct effects in the association and surface active behavior were noted for EB and EBE copolymers (with comparable block lengths and compositions). The EB copolymers (i) have lower critical micelle concentrations (cmc) and (ii) form micelles with larger size and association number than EBE copolymers.[9−13] The lengthening of the E block with fixed B part led to a large decrease in the cmc values for diblock EB copolymers[14−16] and while cmc's were increased for triblock

* To whom correspondence may be addressed. E-mail: nvsastry_ad1@sancharnet.in.

(1) Piirma, I. *Polymeric Surfactants*; Surfactant Science Series 42; Marcel Dekker: New York, 1992; Chapters 2 and 3, pp 17−84.
(2) Chu, B.; Zhou, Z.-K. Physical Chemistry of Polyoxyalkylene Block Copolymer Surfactants. In *Nonionic Surfactants*. Nace, V. M., Ed.; Surfactant Science Series 60; Marcel Dekker: New York, 1996; Chapter 3, p 67.
(3) Alexandridis, P. *Curr. Opin. Colloid Interface Sci.* **1997**, *2*, 478.
(4) Booth, C.; Attwood, D. *Macromol. Rapid Commun.* **2000**, *21*, 501.
(5) Heatley, F.; Yu, G.-E.; Sun, W.-B.; Pywell, E. J.; Sun, E. J.; Mobbs, R. H.; Booth, C. *Eur. Polym. J.* **1990**, *26*, 583.
(6) Heatley, F.; Yu, G.-E.; Draper, M. D.; Booth, C. *Eur. Polym. J.* **1991**, *27*, 471.
(7) Mai, S.-M.; Booth, C.; Kelarakis, A.; Havredaki, V.; Ryan, A. J. *Langmuir* **2000**, *16*, 181.
(8) *B−Series Polyglycols, Butylene Oxide/Ethylene Oxide Block Copolymers*, technical literature; Dow Chemical Co.: Freeport, TX, 1994.
(9) Nace, V. M. *J. Am. Oil Chem. Soc.* **1996**, *73*, 1.
(10) Yang, Z.; Pickard, S.; Deng, N.-J.; Barlow, R. J.; Attwood, D.; Booth, C. *Macromolecules* **1994**, *27*, 2371.
(11) Yang, Y.-W.; Deng, N.-J.; Yu, G.-E.; Zhou, Z.-K.; Attwood, D.; Booth, C. *Langmuir* **1995**, *11*, 4703.
(12) Yu, G.-E.; Yang, Y.-W.; Yang, Z.; Attwood, D.; Booth, C.; Nace, V. M. *Langmuir* **1996**, *12*, 3404.
(13) Chaibundit, C.; Mai, S.-M.; Heatley, F.; Booth, C. *Langmuir* **2000**, *16*, 9645.
(14) Bedells, A. D.; Arafeh, R. M.; Yang, Z.; Attwood, D.; Heatley, F.; Pedget, J. C.; Price, C.; Booth, C. *J. Chem. Soc., Faraday Trans.* **1993**, *89*, 1235.
(15) Kelarakis, A.; Havredaki, V.; Yu, G.-E.; Derici, L.; Booth, C. *Macromolecules* **1998**, *31*, 944.

10.1021/la027072j CCC: $25.00
Published on Web 05/02/2003

EBE copolymers.[4,12,16] Kelarakis et al.[15,16] have observed that the area adsorbed per diblock EB copolymer molecule at the air/water interface becomes 1.6 times larger when E block length is almost doubled. The micelles of diblock EB copolymers have been reported to be bigger in size only when the parent copolymer has a longer E block ($>E_{38}$).[14,16−19] On the other hand, among $E_{18}B_{10}$ and $E_{24}B_{10}$ copolymers,[12,14] the micelles of the latter were found to be smaller in size over the micelles of the former. No such trends were noted in the dependence of the hydrodynamic radius, R_h, on the E block length for the triblock EBE copolymer micelles.[4,12] The micellar association number, $\check{n}$, at a fixed temperature always found to decrease drastically when E block is lengthened irrespective of EB or EBE micelles.[4,11,12,14,16−19]

The effect of temperature on R_h and $\check{n}$ of di- and triblock copolymer micelles has been monitored by Booth and coworkers.[11,12,14,16−22] The rise in the temperature did not produce significant changes in the R_h values, but at the same time the micellar associates could accommodate more copolymer molecules. In all these studies, the authors treated the data assuming spherical shape for the micelles. The question, whether the micelles of EB copolymers at elevated temperatures retain the same shape or not, has been addressed using small angle neutron scattering (SANS) measurements on $E_{90}B_{10}$, $E_{40}B_{10}$, and $E_{18}B_{10}$ micelles in dilute aqueous solutions.[18,23] Derici et al.[18] noted that $E_{90}B_{10}$ copolymer micelles are spherical in shape with the homogeneous core attached with Gaussian chains in the temperature range of 20−70 °C. However, Hamley et al.[23] reported that the micelles of the short chain containing $E_{18}B_{10}$ copolymer become wormlike in the temperature range of 40−50 °C from initial spherical geometry at 20 °C.

In view of the scarce and nonconsistent information available on the structural characteristics of EB and EBE copolymer micelles, we have recently taken up detailed studies of the phase, surface active, and micellar behavior of two commercially available copolymers (i.e., $E_{18}B_9$ and $E_{13}B_{10}E_{13}$) using SANS and viscosity data.[24] As part of our ongoing program to evaluate the structural characteristics of the micelles of polymeric surfactants, we report detailed investigations on the surface active, association, and phase behavior of a diblock B_9E_{16} and triblock $E_{43}B_{14}E_{43}$ copolymer in aqueous solutions. The micellar behavior and the temperature-induced changes in the micellar structure have been monitored from dynamic light scattering (DLS) and viscosity measurements in solutions of varying copolymer concentrations and at different temperatures.

2. Experimental Section

2.1. Copolymers. The block copolymers were obtained as gift samples from The Dow Chemical Company, Freeport, TX. They were used as received. The diblock copolymer BL-50 has structure of type $C_4H_9O-(BO)_n-(EO)_m-OH$, with $m = 16$ and $n = 9$ units, while the triblock copolymer, B-20 has structure $HO-(EO)_m-(BO)_n-(EO)_m-OH$, with $m = 43$ and $n = 14$ units. EO and BO in the structures represent oxyethylene and oxybutylene units. The di- and triblock copolymers have been denoted as EB-1 and EB-2 throughout the study.

2.2. Methods. The surface tension of copolymer solutions was measured by the drop weight method using a modified stalagmometer.[25]

The light scattering apparatus consisted of a laboratory goniometer with two arms. One of these arms housed the excitation source, which was a solid-state frequency-doubled Nd:YAG laser radiating at a wavelength of 532 nm. The DLS experiments were carried out at a fixed scattering angle of 90°. The other arm of the goniometer had the photomultiplier tube mounted onto it enabling angle dependent detection of scattered light. Surfactant solutions were ultracentrifuged at ∼10000 rpm for about half an hour and then directly loaded into an optical quality 5 mL borosilicate cell and sealed. Then the cell was held inside a homemade temperature controller.[26] This controller provided temperature regulation in the range of 15−75 °C with an accuracy of ±0.1 °C. Scattered light from sample solutions was detected by the photomultiplier tube, and the photocurrent was suitably amplified and digitized before it was fed to a 1024 channel digital correlator (Brookhaven Instruments Inc., USA, model BI-9000AT). The whole scattering apparatus was placed on a vibration isolation table (Newport Corp., USA). The correlation spectra were recorded at different temperatures. In all experiments, the difference between the measured and calculated baseline was not allowed to go beyond ±0.1%. The data that showed excessive baseline difference were rejected. All the data exhibited a single narrow distribution. The unimodal particle sizes were determined through the CONTIN[27] software provided by Brookhaven.

The flow times of surfactant solutions and water were obtained by using Ubbelohde suspended level viscometers. Two viscometers were used to record flow times in the range of 130−360 s, thus avoiding any kinetic corrections. Shear corrections were not taken into consideration because obtained intrinsic viscosities were always less than 3 dL g^{-1}. The flow volume was greater than 5 mL, making drainage corrections unimportant. Viscometers were suspended in ISREF, India, thermostatic water baths maintained at constant temperature accurate to ±0.01 °C.

The densities of aqueous surfactant solutions were measured by using a high-precision Anton Paar densitymeter, DMA 5000. The measured densities are accurate to ±0.000001 g cm^{-3}, and the temperature in the measuring cell was maintained to an accuracy of ±0.001 °C by inbuilt integrated Pt 100 measuring sensors.

3. Results and Discussions

3.1. Critical Micelle Concentrations (cmc) and Surface Active Properties. cmc values were obtained from the plots of surface tension versus logarithmic concentrations of copolymer solutions. Such plots are shown in parts a and b of Figure 1. It can be seen that the plots are of "L" type with an initial continuous decrease in surface tension up to a characteristic concentration beyond which the value attains a limiting value. An interpolation between the two straight lines drawn from both the regions was made to extract the exact break points in each plots. These break points are considered as cmc. We did not notice any minima in the crossover region of the plots. Though the working unit of concentrations is g dL^{-1}, the same was converted into mol dm^{-3} by using the total molecular weights of respective copolymers. Our experimental cmc values (together with some literature

(16) Kelarakis, A.; Havredaki, V.; Derici, L.; Yu, G.-E.; Booth, C.; Hamley, I. W. *J. Chem. Soc., Faraday Trans.* **1998**, *94*, 3639.
(17) Deng, N.-J.; Luo, Y.-Z.; Tanodekaew, S.; Bingham, N.; Attwood, D.; Booth, C. *J. Polym. Sci., Part B: Polym. Phys.* **1995**, *33*, 1085.
(18) Derici, L.; Ledger, S.; Mai, S.-M.; Booth, C.; Hamley, I. W.; Pedersen, J. S. *Phys. Chem. Chem. Phys.* **1999**, *1*, 2773.
(19) Mingvanish, W.; Mai, S.-M.; Heatley, F.; Booth, C.; Attwood, D. *J. Phys. Chem. B* **1999**, 103, 11269.
(20) Yu, G.-E.; Ameri, M.; Yang, Z.; Attwood, D.; Booth, C. *J. Phys. Chem. B* **1997**, *101*, 4394.
(21) Yu, G.-E.; Mistry, D.; Ludhera, S.; Heatley, F.; Attwood, D.; Booth, C. *J. Chem. Soc., Faraday Trans.* **1997**, *93*, 3383.
(22) Tanodekaew. S.; Pannu, R.; Heatley, F.; Attwood, D.; Booth, C. *Macromol. Chem. Phys.* **1997**, *198*, 927.
(23) Hamley, I. W.; Pedersen, J. S.; Booth, C.; Nace, V. M. *Langmuir* **2001**, *17*, 6386.
(24) Soni, S. S.; Sastry, N. V.; Patra, A. K.; Joshi, J. V.; Goyal, P. S. *J. Phys. Chem. B* **2002**, *106*, 13069.
(25) Soni, S. S.; Sastry, N. V.; Aswal, V. K.; Goyal, P. S. *J. Phys. Chem. B* **2002**, *106*, 2607.
(26) Bohidar, H. B.; Berland, T.; Jassang, T.; Fedex, J. *Rev. Sci. Instrum.* **1987**, *58*, 1422.
(27) Provencher, S. W. *Comput. Phys. Commun.* **1982**, *27*, 213. Provencher, S. W. *Comput. Phys. Commun.* **1979**, *27*, 227. Provencher, S. W. *Makromol. Chem.* **1979**, *180*, 201.

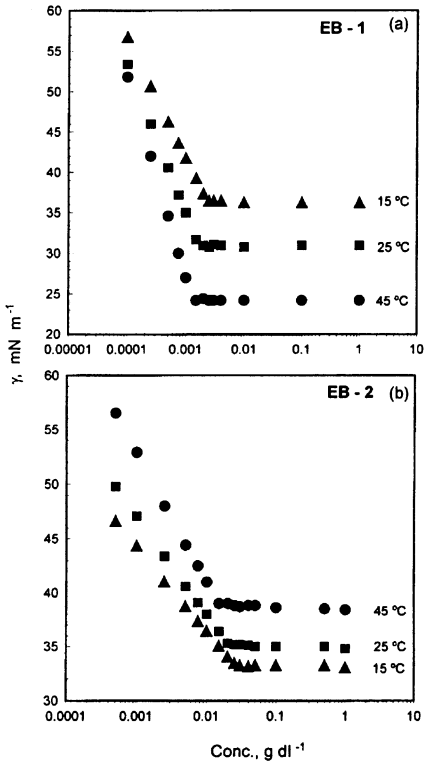

Figure 1. Plots of surface tension versus logarithm concentration for (a) EB-1 and (b) EB-2 copolymer aqueous solutions at different temperatures.

available data) in mol dm^{-3} along with several other useful surface active properties deduced from the plots of Figure 1 are listed in Table 1. These properties include surface excess concentration, Γ_m, of copolymer molecules in the surface layer compared to the bulk, the surface area per molecule, a_1^s, in the surface monolayer, and the concentration at which surface tension of water was reduced by 20 units, C_{20}. The maximum surface pressure, π_{cmc}, Γ_m, and a_1^s were calculated using standard procedures.[28]

As far as we are aware, there are no literature reports on the temperature dependence of cmc and other surface active properties for the B_9E_{16} and $E_{43}B_{14}E_{43}$ copolymers. A perusal of data in column 2 of Table 1 clearly shows that cmc's almost become a little less than half of their values when the temperature is raised from 15 to 45 °C. The comparison of our interpolated cmc's (in mol dm^{-3}) of 0.925×10^{-5} (for B_9E_{16} at 40 °C) and 3.70×10^{-5} (for $E_{43}B_{14}E_{43}$ at 30 °C) with the literature data of 1.099×10^{-4} (for $E_{49}B_8$ at 40 °C)[14] and 3.585×10^{-5} (for $E_{105}B_{15}E_{105}$ at 30 °C)[16] reveals that the lengthening of hydrophilic chains causes drastic increase in cmc value in diblock copolymers, while the change in the same is the bare minimum for triblock copolymers. Thus molecular architecture plays a decisive role as far as micellization ability of these copolymers is concerned. One can normally expect that the copolymer molecules with a longer hydrophilic chain cover more surface area, and we indeed notice this trend as our interpolated a_1^s value of 41.5 $Å^2$ for B_9E_{16} at 40 °C is smaller than the area of 64 $Å^2$ at 40 °C for $E_{41}B_8$ copolymer.[10] The rise in temperature would induce more thermal motion in the hydrophilic chains and also cause dehydration, and hence the observed continuous decrease in a_1^s values with the temperature rise for the molecules of both the copolymers is justifiable. A similar decreasing trend in a_1^s values was noted for $E_{50}B_{13}$ and $E_{106}B_{16}$ copolymers in the temperature range 20−50 °C.[14,15]

3.2. Thermodynamic Parameters of Micellization. The free energy of micellization, $\Delta G°_{Mic}$, values at different temperatures were calculated using the standard relation.[28] The $\Delta G°_{Mic}$ values at different temperatures were fitted to a linear relation to estimate the enthalpy, $\Delta H°_{Mic}$, and entropy, $\Delta S°_{Mic}$, of micellization. The last three columns of Table 1 list the values for the above parameters. It can be seen that the $\Delta H°_{Mic}$ is positive, i.e., endothermic, while the $\Delta G°_{Mic}$ is large and negative for both the copolymer micelles. Hence, the deciding factor that favors the association is the positive $\Delta S°_{Mic}$. $\Delta G°_{Mic}$ values for the diblock copolymer are slightly more negative than those obtained for the triblock copolymer. Since the diblock copolymer B_9E_{16} has 3.5 times higher hydrophobic to hydrophilic part ratio than $E_{43}B_{14}E_{43}$, the molecules of the former enter into association with greater ease than the molecules of the latter.

3.3. Association Behavior and Micellar Properties. An attempt has been made to elicit information on the micellar structural characteristics especially micellar size and geometry for the di- and triblock copolymer micelles using dynamic light scattering measurements. Various solutions in the concentration range 1−10 g dL^{-1} of B_9E_{16} and $E_{43}B_{14}E_{43}$ copolymers were studied in the temperature range of 30−70 °C. The results were analyzed using CONTIN regression software[29] provided by Brookhaven Instruments (BIC, USA). This analysis is specifically aimed at estimating the average translational diffusion coefficient, $\bar{D}$, from the measured intensity autocorrelation function and the concentration dependence of $\bar{D}$ can be written as[29]

$$\bar{D} = \bar{D}_o(1 + k_D C) \tag{1}$$

where k_D is a parameter characteristic of micellar interactions and $\bar{D}_o$ is the *z*-average diffusion coefficient at infinite dilution. The translational friction coefficient f_t was estimated through Einstein's relation

$$\bar{D}_o = k_B T/f_t \tag{2}$$

where k_B is the Boltzmann constant and T is the absolute temperature.

The usage of Stokes law or the Tanford[30] expression leads to information on the shape and size of the micelles. For example, as per the Stokes law, if the associates are spherical, f_t will be equal to $6\pi\eta R_h$, where R_h is the hydrodynamic radius of associates. When the associates are nonspherical, f_t can be related to characteristic semimajor and semiminor axes of **b** and **a** for the prolate and oblate ellipsoids of revolution through the relations

prolate ellipsoid

$$f_t = \frac{6\pi\eta\mathbf{b}(1 - \mathbf{a}^2/\mathbf{b}^2)^{1/2}}{\ln\left[\dfrac{1 + (1 - \mathbf{a}^2/\mathbf{b}^2)^{1/2}}{\mathbf{a}/\mathbf{b}}\right]} \tag{3}$$

and

(28) Rosen. M. J. *Surfactants and Interfacial Phenomena*, 2nd ed.; John Wiley and Sons: New York, 1989; Chapters 2, 3, and 5.

(29) Pecora, R. *Dynamic Light Scattering*; Plenum: New York, 1985.

(30) Tanford, C. *Physical Chemistry of Macromolecules*; Wiley: New York, 1961; 327 pp.

Table 1. Values of cmc, C_{20}, cmc/C_{20}, Surface Excess Concentration, Γ_m, Area per Copolymer Molecule, a_1^s, Surface Tension at cmc, γ_{cmc}, Maximum Surface Pressure, π_{cmc}, Free Energy, $\Delta G°_{Mic}$, Enthalpy, $\Delta H°_{Mic}$, and Entropy, $\Delta S°_{Mic}$, of Micellization for Copolymer Micelles at Different Temperatures

temp (°C)	cmc (mol dm^{-3})	C_{20} (mol dm^{-3})	cmc/C_{20}	$10^{10}\Gamma_m$ (mol cm^{-2})	a_1^s (Å^2)	γ_{cmc} (mN m^{-1})	π_{cmc} (mN m^{-1})	$\Delta G°_{Mic}$ (kJ mol^{-1})	$\Delta H°_{Mic}$ (kJ mol^{-1})	$\Delta S°_{Mic}$ (kJ K^{-1} mol^{-1})
					EB-1					
15	$(1.5 \pm 0.1) \times 10^{-5}$	5.9×10^{-7}	25	2.7 ± 0.2	62 ± 1	32.1 ± 0.2	41.3 ± 0.2	-36.2 ± 1.8		
25	$(1.3 \pm 0.1) \times 10^{-5}$	8.0×10^{-7}	16	3.2 ± 0.2	52 ± 2	31.8 ± 0.4	40.0 ± 0.4	-38.1 ± 1.8		
	1.2×10^{-5} [a]			3.3[a]	51[a]					
45	$(0.8 \pm 0.2) \times 10^{-5}$	1.6×10^{-6}	5	4.4 ± 0.2	38 ± 1	29.2 ± 0.3	39.4 ± 0.3	-41.6 ± 2.2		
									17.5 ± 0.9	0.19 ± 0.01
					EB-2					
15	$(5.0 \pm 0.4) \times 10^{-5}$	2.6×10^{-7}	192	1.4 ± 0.2	117 ± 1	33.1 ± 0.2	40.3 ± 0.2	-33.3 ± 1.7		
25	$(4.0 \pm 0.3) \times 10^{-5}$	5.3×10^{-7}	76	1.6 ± 0.2	105 ± 2	35.2 ± 0.3	36.6 ± 0.3	-35.0 ± 1.8		
	4.0×10^{-5} [a]			1.6 [a]	107[a]					
45	$(2.8 \pm 0.2) \times 10^{-5}$	4.7×10^{-6}	6	1.9 ± 0.2	87 ± 1	38.4 ± 0.3	30.2 ± 0.3	-38.3 ± 2.1		
									14.6 ± 0.8	0.17 ± 0.01

[a] From ref 9.

oblate ellipsoid

$$f_t = \frac{6\pi\eta\mathbf{a}(\mathbf{b}^2/\mathbf{a}^2 - 1)^{1/2}}{\tan^{-1}(\mathbf{b}^2/\mathbf{a}^2 - 1)^{1/2}} \quad (4)$$

Thus preassuming a particular shape for the associates and giving trial values to the micellar dimensions in an iterative manner, the experimental values of f_t were reproduced.

The plots showing the dependence of $\bar{D}$ on the concentrations of copolymers at different temperatures are given in Figure 2. The extrapolation of $\bar{D}$ to zero concentration yielded the $\bar{D}_o$ values. The various micellar parameters derived from the above analysis are summarized in Table 2. The micelles of the EB-1 diblock copolymer at 30 and 45 °C and of the EB-2 triblock copolymer at 30, 50, and 70 °C are found to be spherical in shape with a polydispersity value of 0.53. The micelles thus consist of a spherical hydrophobic core with an outer shell of water swollen hydrophilic chains. Another common feature that could be seen is that the hydrodynamic radius, R_h, increases with the rise in temperature for the micelles of both the copolymers. As far as we are aware, there is no literature information on the micelles of EB-1 diblock copolymer. The rise in the temperature is expected to decrease the swelling of the outer hydrophilic shell of the micelles due to dehydration effects and also would expand the hydrophobic core part. It is essentially the balance of these two opposing effects that would influence the overall hydrodynamic size of the micelles with temperature changes. In a recent paper,[24] we have reported systematic SANS investigations on $H_3C-O-(E)_{18}-(B)_9-OH$ micelles and it has been indeed found that micelles are hard spherical in shape and both the core and hard sphere interaction radii increase with the temperature rise from 30 to 40 °C. There are several reports in the literature where the R_h value has been found to increase with temperature for E_mB_n,[11,14] $E_mB_nE_m$,[11] E_mP_n,[31] and $E_mP_nE_m$[32,33] copolymer micelles.

Strikingly, the spherical micelles of EB-1 diblock copolymer turn in to prolate ellipsoidal shape as the temperature is raised from 45 to 60 °C with considerable decrease in the polydispersity value. The distortion of the shape has been found to be so drastic that the micelles at 60 °C have a semimajor axis length of 135 Å and an axial ratio of 3.2. The latter value is about three times higher

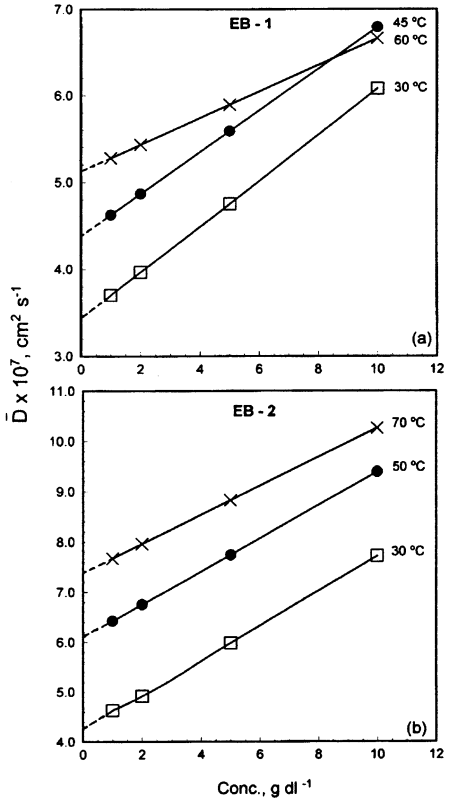

Figure 2. Plots of translational diffusion coefficient versus concentration for (a) EB-1 and (b) EB-2 copolymer micelles at different temperatures.

considering an axial ratio of 1.0 for a spherical shape. The reason for the transition from spherical to ellipsoidal in the case of EB-1 copolymer micelles at 60 °C needs to be accounted for. The balance between the hydrophobic and hydrophilic portions in EB-1 diblock copolymer is 3.5 times more than the same for the EB-2 copolymer. The distortion in spherical shape of the block copolymer micelles at elevated temperatures has been usually attributed to the dehydration of associates.[24,25,34−39] Our recent SANS analysis of 2 wt % (w/v) solution of $H_3C-O-(E)_{18}-(B)_9-OH$ revealed that the spherical micelles of the copolymer turn to prolate ellipsoidal at 50 °C with large

(31) Altinok, H.; Nixon, S. K.; Gorry, P. A.; Attwood, D.; Booth, C.; Kelarakis, A.; Havredaki, V. *Colloid Surf., B* **1999**, *16*, 73.
(32) Zhou, Z. −K.; Chu, B. *Macromolecules* **1988**, *21*, 2548.
(33) Zhou. Z. −K.; Chu, B. *J. Colloid. Interface Sci.* **1988**, *126*, 171.
(34) Guo, C.; Liu, H. Z.; Chen, J. Y. *Colloid Polym. Sci.* **1999**, *277*, 376.
(35) Goldmints, I.; von Gottberg, F. K.; Smith, K. A.; Hatton, T. A. *Langmuir* **1997**, *13*, 3659.
(36) Goyal, P. S.; Menon, S. V. G.; Dasannacharya, B. A.; Thiyagarajan, P. *Phys. Rev. E* **1995**, *51*, 2308.

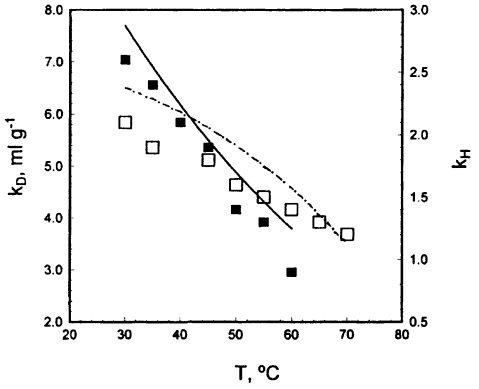

Figure 3. Variation of interaction parameters, k_D, and Huggins constant, k_H, with temperature. Lines correspond to k_D and points correspond to k_H: (—) and (■) for EB-1; (- - -) and (□) for EB-2 copolymers.

Table 2. Average Translational Diffusion Coefficient at Infinite Dilution, $\bar{D}_o$, Polydispersity, *P*, Hydrodynamic Radius, R_h, Semimajor Axis, *b*, Semiminor Axis, *a*, Axial Ratio, *b*/*a*, for EB and EBE Block Copolymer Micelles at Different Temperatures

Spherical Model			
temp (°C)	$10^7\bar{D}_o$ (cm^2 s^{-1})	P	R_h (Å)
	EB-1		
30	3.4 ± 0.2	0.42	81 ± 3
45	4.4 ± 0.3	0.32	89 ± 2
	EB-2		
30	4.4 ± 0.3	0.53	64 ± 4
			62 ± 3[a]
50	6.1 ± 0.4	0.41	71 ± 3
70	7.4 ± 0.4	0.44	84 ± 4

Prolate Ellipsoidal Model, EB-1					
temp (°C)	$10^7\bar{D}_o$ (cm^2 s^{-1})	*b* (Å)	*a* (Å)	*b*/*a*	P
60	5.1 ± 0.2	135 ± 5	42 ± 2	3.2	0.25

[a] From ref 12.

changes in micellar association number and number density of micelles.[24]

3.4. Micellar Interactions. The parameters k_D and k_H obtained from the slope values of eq 1 and Huggins relation, $\eta_{sp}/C = [\eta]\{1 + k_H[\eta]C\}$ (where, η_{sp}, $[\eta]$, and C are the specific viscosity, intrinsic viscosity, and copolymer concentration, respectively), are a measure of the net interactions in the micelles due to the thermodynamic and hydrodynamic factors. The parameter k_D in fact is related[40] to the thermodynamic second virial coefficient, A_2, and the frictional coefficient, f_t, through the relation $k_D = 2A_2\bar{M}_w - f_t - \bar{v}$, where $\bar{M}_w$ is the micellar molar mass. Since the micelles of EB-1 and EB-2 copolymers are found to be compact with very small spatial extension, the overall contribution of f_t to k_D can be ignored. Thus the sign of k_D depends only on the sign of A_2 which in turn depends on intramicellar interactions. The variations of k_D and k_H for the EB-1 and EB-2 copolymer micelles with temperatures are shown in Figure 3. The k_D and k_H values are positive and in sign agreement with each other. A definite decreasing trend in both k_D and k_H values has been recorded with the rise in temperature. The large positive k_D and k_H values at 30 °C indicate the pronounced repulsive interactions (between the hydrophobic part of the copolymer and water) and the same get weakened at elevated temperatures. So, at higher temperatures one would expect that the repulsive interactions will be replaced by attractive forces (i.e., better cohesion among the copolymer solute−solute and solute−water molecules). This situation leads to the micellar growth in terms of size, association number, and also enhanced number density of micelles.

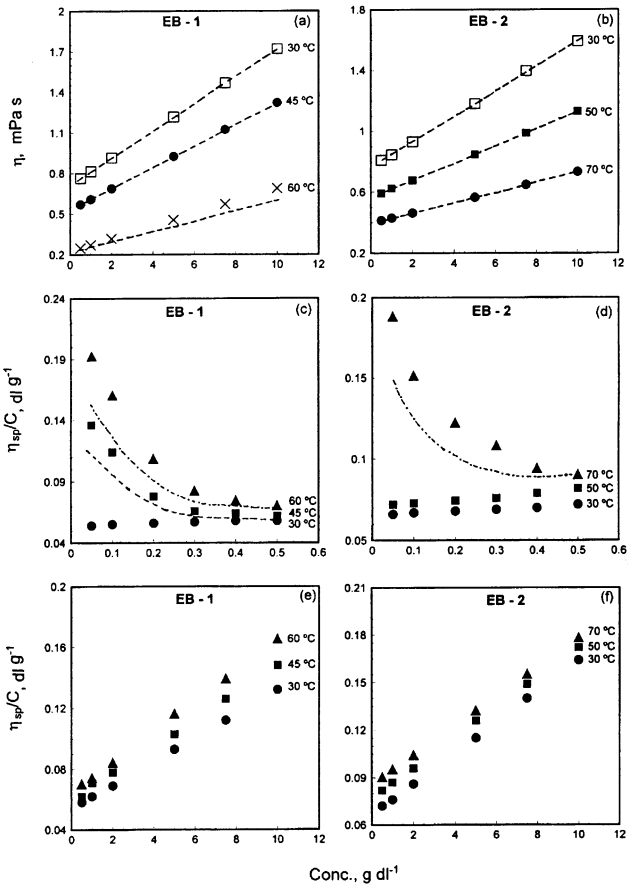

Figure 4. (a and b) Absolute viscosity vs concentration profiles at different temperatures for aqueous solutions of EB-1 and EB-2 copolymers, respectively. Dashed lines are the theoretical values calculated assuming spherical shape for the micelles. (c−f) Concentration dependence of reduced viscosities for aqueous solution in (c and d) very dilute concentration range and (e and f) dilute to moderate concentration range. Points are experimental values, and the dashed curves (in parts c and d) are calculated using eq 5 at different temperatures.

3.5. Dilute Solution Viscosity of Micellar Solutions. The viscosity measurements on micellar solutions provide very useful information on the shape, hydrodynamic volume, and hydration. The variation of experimentally measured absolute viscosities of EB-1 and EB-2 copolymer solutions over the concentration range of 1−10 wt % (w/v) and at different temperatures is shown in parts a and b of Figure 4. Considering that the micelles are spherical in shape at three temperatures, we have attempted to calculate the theoretical viscosities, η, using Einstein's formula $\eta = \eta_o(1 + 2.5\phi)$, where ϕ is the volume fraction of copolymer in the solution and η_o is the absolute viscosity of copolymer solution at cmc. Thus obtained values are shown as dotted lines in Figure 4. Excellent agreement between the experimental and theoretical viscosities for EB-1 copolymer solutions at 30 and 45 °C and for EB-2 copolymer solutions at 30, 50, and 70 °C has been found (the root-mean-square standard deviation, σ, between the experimental and theoretical values ranged from 0.002 to 0.003 mPa s). However, as expected, Einstein's formula meant for hard spheres could not be applied to prolate

(37) Liu, Y. C.; Chen, S. H.; Huang, J. S. *Physica B* **1998**, *243*, 1019.
(38) Mortensen, K.; Pedersen, J. S. *Macromolecules* **1993**, *26*, 805.
(39) Hvidt. S.; Jorgensen, E. B.; Brown, W.; Schillen, K. *J. Phys. Chem.* **1994**, *98*, 12320.
(40) Vink, H. *J. Chem. Soc., Faraday Trans. 1* **1985**, *81*, 1725.

ellipsoid micelles of EB-1 copolymer at 60 °C, and the σ values, as expected, have been found to be as large as 0.182 mPa s.

The dependence of reduced viscosities, η_{sp}/C, on the copolymer concentrations for both EB-1 and -2 in very dilute as well as dilute solutions at different temperatures is shown in parts c−f of Figure 4. A perusal of the profiles in very dilute solutions (concentration range 0.05−0.5 g dL^{-1}) (parts c and d of Figure 4) shows an interesting trend. η_{sp}/C values for EB-1 solutions at 30 °C and for EB -2 solutions at 30 and 50 °C are typical in which they increase gradually in a linear manner as expected from the well-known Huggins equation. The same profiles at elevated temperatures have shown a rectilinear nature with large increase of the reduced viscosity values in very dilute solution range. We have also noticed such complex nature for $H_3C-O-(E)_{18}-(B)_9-OH$ and $OH-(E)_{13}-(B)_{10}-(E)_{13}-OH$ copolymer solutions,[24] as noted by Kelarakis et al.[41] for hydroxy- and methoxy-ended $(E)_{18}(B)_{10}$ copolymer solutions. Such sharp shoot up of η_{sp}/C values in the very low concentrations was attributed to the adsorption of copolymer molecules on the capillary wall of viscometer during the flow. Thus the measured η_{sp}/C values under these conditions are apparent, and Ohrn[42] related them with the real values through the relation

$$(\eta_{sp}/C)^* = \eta_{sp}/C + \Delta \qquad \text{and} \qquad \Delta \approx (\eta_r/C)(4a_{lay}/r) \quad (5)$$

where the asterisk indicates the apparent value. The terms η_r, a_{lay}, and r are the relative viscosities, thickness of adsorbed layer, and radius of the capillary of the viscometer used (0.300 mm in the present case). We have tried to reproduce the trend in very dilute solution η_{sp}/C values by using the Ohrn relation, and they are shown as dashed lines in parts c and d of Figure 4. The calculation further showed that the adsorbed layer thickness a_{lay} is equal to 300−400 nm. The observed adsorption effects at elevated temperatures of 45−70 °C are attributable to the fact that the copolymer molecules become relatively more hydrophobic with the rise in temperature due to dehydration effects. The adsorption effects, as expected, become negligible at room temperature and as the concentration of copolymers is increased.

The η_{sp}/C vs C plots (shown in parts e and f of Figure 4) were used to get the intrinsic viscosity, $[\eta]$, values. The $[\eta]$ values for the micelles of both the copolymers at different temperatures are listed in column two of Table 3. It can be seen that the $[\eta]$ values gradually increase with rise in temperature irrespective of type of chain architecture. The enhanced $[\eta]$ values at elevated temperatures indicate the enlarged hydrodynamic volume of the micelles. This is consistent with our earlier observation that the micelles grow in size with the rise in the temperature.

3.6. Hydration of Micelles. The hydration, W, in terms of grams of water to grams of copolymer in micellar solutions has been widely obtained by[43,44]

$$W = \tilde{v}\rho_o\{(100[\eta]/2.5\tilde{v}) - 1\} \quad (6)$$

where $\tilde{v}$, ρ_o, and $[\eta]$ are the partial specific volume of copolymer, density of water, and intrinsic viscosity, respectively. The $\tilde{v}$ values were calculated from the slopes of the linear plots as per the equation $\rho = \rho_o + (1 - \tilde{v}\rho_o)C$,

Table 3. Intrinsic Viscosity, $[\eta]$, Partial Molar Volume, $\tilde{v}$, Hydration, W, and Number of Water Molecules per Copolymer Molecule and EO Group for EB and EBE Block Copolymer Micelles at Different Temperatures

				no. of water molecules per	
temp (°C)	$[\eta]$ (mL g^{-1})	$\tilde{v}$ (mL g^{-1})	W (g of H_2O/ g of copolymer)	copolymer molecule	EO group
			EB-1		
30	5.43	0.9435	1.22	102	6.4
35	5.34	0.9525	1.14	95	5.9
40	5.65	0.9574	1.09	91	5.7
45	5.85	0.9622	1.02	84	5.3
50	6.15	0.9664	0.97	81	5.1
55	6.25	0.9717	0.85	71	4.4
60	6.60	0.9743	0.74	61	3.8
			EB-2		
30	6.75	0.8748	1.82	505	5.9
35	6.80	0.8838	1.75	485	5.6
45	7.03	0.8929	1.63	453	5.3
50	7.08	0.8968	1.58	437	5.1
55	7.14	0.9029	1.52	421	4.9
60	7.25	0.9089	1.48	411	4.8
65	7.35	0.9130	1.42	394	4.5
70	7.90	0.9181	1.35	375	4.3

where ρ is the density of solution at a given concentration. The $\tilde{v}$ and W values as a function of temperature for the solutions of both the copolymers are given in columns three and four of Table 3. The last two columns of the table are derived from W values. The notable and worthy feature of the W data is that the hydration values continuously show a decrease with the rise in temperature. The maximum decrease is 1.6 times (temperature range 30−60 °C) and 1.3 times (temperature range 30−70 °C) for EB-1 and EB-2 copolymer micelles, respectively. The dehydration effect would thus provide a favorable inner dry micellar environment so that the hydrophobic core part stretches and result in the increased micellar size at elevated temperatures. Dehydration of micelles at higher temperatures of di- and triblock EP and EPE copolymers has also been documented in the literature.[35−37] A look at the last column of the Table 3 reveals that the number of water molecules per oxyethylene unit ranges between 3.8 and 6.4 at elevated temperatures to 30 °C. It has been found by the use of calorimetric measurements of heat of mixing that at low polymer concentrations, each oxyethylene unit in polyoxyethylene bonds at a molar ratio of two water molecules to one oxyethylene.[1,45] Thus, it can be stated that the hydrophilic shell of micelles of EB-1 and EB-2 copolymers has to be profusely swollen with additional water molecules at 30 °C, which are pushed out at elevated temperatures. But the outer shell of the micelles still holds sufficient water molecules (>2 in number) at 60 and 70 °C for EB-1 and EB-2 copolymer micelles, respectively.

3.7. Dilute Solution Phase Diagrams. One of the characteristic features of the amphiphilic di- and triblock EP, EPE, EB, and EBE copolymers, etc., is that their aqueous solutions, when warmed, turn turbid and cloudy.[9] Though the exact and universal definition of cloud point and explanation for the unique phase behavior of the copolymer solutions are still to emerge, the growth of micellar associates, dehydration, and enhanced attractive intramicellar interactions can be considered for a plausible understanding of the phase behavior. The dilute solution phase diagrams for EB-1 and EB-2 copolymers are depicted in parts a and b of Figure 5. Though, some common features are observed, we noticed distinct differences in the

(41) Kelarakis, A.; Havredaki, V.; Booth, C.; Nace, V. M. *Macromolecules* **2002**, *35*, 5591.
(42) Ohrn, O. E. *J. Polym. Sci.* **1955**, *17*, 137.
(43) Tokiwa, F.; Ohki, K. *J. Phys. Chem.* **1967**, *71*, 1343.
(44) Oncley, J. L. *Ann. N. Y. Acad. Sci.* **1949**, *41*, 121.
(45) Schott, H. *J. Chem. Eng. Data* **1966**, *11*, 417.

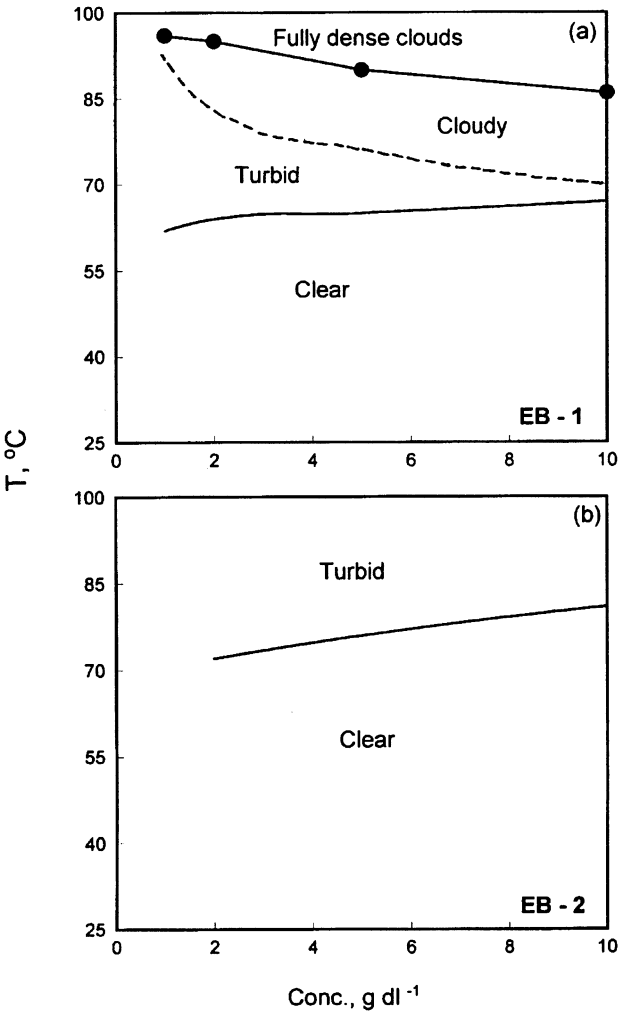

Figure 5. Phase diagrams for (a) EB-1 and (b) EB-2 copolymers in dilute aqueous solutions. (●) Final cloud points for respective concentrations of copolymer solutions.

solutions (1−10 wt % (w/v) concentrations) of EB-1 and EB-2 copolymer. Upon initial warming, the clear solutions turn turbid (appearance of milkiness but still transparent). The EB-1 diblock copolymer solutions become cloudy (development of haziness from the top portion and the solutions are no longer transparent, i.e., one cannot see through them) with further warming before resulting into dense clouds throughout the solution volume at elevated temperatures. The dense clouds, once formed, remained stable up to 95 °C. In contrast to this, we could not see any cloudiness in EB-2 triblock copolymer solutions even at temperatures as high as 95−97 °C. Also, in comparison to EB-1 solutions, the region through which the solutions remained clear is far wider in EB-2 solutions. We attribute the temperature at which dense clouds are formed to cloud point. Our observed initial turbidity and cloud points of 62 (63[9]) and 95 (99[9]) °C for 1 wt % (w/v) solutions of EB-1 copolymer match well with the literature values. As the concentration of both the copolymers is increased, the turbidity has been observed to set in at slightly higher temperatures (as shown by the dashed boundary lines in parts a and b of Figure 5). The possibility that EB-2 solutions may have cloud points beyond 100 °C and its solutions remain in general clear up to higher temperatures clearly shows the importance of net balance of hydrophobic to hydrophilic portions in the copolymer molecules. In EB-2 copolymer, this balance is strongly in favor of the former, and in EB-1 copolymer, the same is equally balanced between the two parts. Thus, the dehydration effects at elevated temperatures decrease the miscibility (and or solubility) of both the hydrophobic and hydrophilic parts with water.

Other factors such as our observed increase in micellar size, distortion of shape, and enhanced intramicellar interactions do contribute to the appearance of turbidity and cloudiness in the solutions. The fact that the EB-2 copolymer aqueous solutions (1−10 wt % (w/v)) are clear with spherical micelles at 70 °C demonstrates that the observed turbidity and eventual cloudiness in EB-1 copolymer solutions would have significant contributions from the asymmetrically shaped large micelles at temperatures beyond 60 °C.

Conclusions

The critical micelle concentration and surface active properties such as surface excess concentration and area per copolymer molecule at air/water interface have been found to be dependent upon the ratio of overall block composition for oxybutylene and oxyethylene copolymers. The micellization in these copolymers has been found to be an entropy driven process. The micelles of both B_9E_{16} and $E_{43}B_{14}E_{43}$ copolymers are spherical in shape at 30 °C, and the micellar size progressively increases with rise in the temperature. However, the micelles of diblock copolymer in which the balance of block lengths is in favor of hydrophobic oxybutylene chains undergo sphere-to-prolate ellipsoidal transition at higher temperature. Similarly, the triblock EBE copolymer solutions (in the concentration range of 1−10 wt % (w/v)) have cloud points greater than 100 °C, while the solutions of diblock EB copolymer under the same conditions become as usual turbid and cloudy with clear cloud points, since polymeric surfactants do yield micellar solutions with larger particle size distribution and, hence, a larger polydiseprsity. The observed phase behavior demonstrates that it is dictated equally by the type and size of micelles and the proportion of individual block lengths in the given copolymer.

Acknowledgment. One of the authors S.S.S. thanks the IUC-DAEF, Mumbai, for awarding a research assistantship under Grant No. IUC/CRS-M-73/362-66.

LA027072J